A CIRCULAR ELASTIC CYLINDER UNDER EXTENSION

W.-D. Tseng [*]

Department of Civil Engineering
National Cheng Kung University
Tainan, Taiwan 70101, R.O.C.

Department of Construction Engineering
Nan-Jeon Institute of Technology
Tainan, Taiwan 73746, R.O.C.

J.-Q. Tarn [**]

Department of Civil Engineering
National Cheng Kung University
Tainan, Taiwan 70101, R.O.C.

ABSTRACT

Analysis of deformation and stress field in a circular elastic cylinder under the extension is presented, with emphasis on the end effect. The problem is formulated on the basis of the state space formalism for axisymmetric deformation of transversely isotropic materials. A rigorous solution that satisfies the prescribed end conditions is determined by using symplectic eigenfunction expansion, thereby, the applicability of the Saint-Venant solution is examined. The results show that the end effect is significant but confined to a local region near the base of the cylinder where the end plane is perfectly bonded or subjected to a concentrated load. As the axial stiffness increases, the end effect on the stress state increases at the loaded end but decreases at the bonded end. The displacement and stress distributions across the section are uniform throughout the length of the cylinder except near the ends.

Keywords : Circular cylinders, End effects, State space, Symplectic orthogonality.

1. INTRODUCTION

The simplest case of stress distribution in anisotropic cylinders is that of the extension of an axial force applied at its end. The stress and displacement components can be obtained in an elementary way [1,2]. Under axial loading applied at the centroid of the end section, the internal forces in a cylinder are normal to the plane of the section and the corresponding stress is described as a normal stress and the average value of the stress over the cross section is obtained by dividing the resultant of the internal forces by the area of the cross section. If the force is uniformly distributed, the stress is uniform everywhere in the cylinder.

In general, the actual distribution of stresses in any given section is statically indeterminate. In a cylinder subjected to concentrated loads, the stress at a given point of the section may be different from the average value and vary across the section. When a cylinder is bonded to a rigid base, the interface between the end plane and the rigid base imposes certain constraints on the body, which dictate the end conditions. Saint-Venant's principle makes it possible to replace a given loading by the average value. The normal stresses can be assumed uniformly distributed in any cross section; however, such an assumption may be quite in error in the immediate vicinity of the points of the applied loads and at the bonded end. To learn more about their distributions, it is necessary to consider the deformations resulting from the actual distribution of the prescribed loads and the end conditions at both ends of the cylinder. Rigorous analytic or experimental methods must be used to determine the distribution of stresses in these areas. An exact analysis of this problem is not so simple as it appears.

In this paper we present an exact analysis of the displacement and stress fields in a circular elastic cylinder under extension. The state space formalism is used to determine the distribution of stresses corresponding to a concentrated load at the end of the cylinder. When the material is transversely isotropic with the axis being the axis of rotational symmetry, the problem is axially symmetric. It is well known that the axisymmetric problem can be formulated by stress function approach [2] to reduce the basic equations to a biharmonic-type governing equation, yet the BC in terms of the unknown function are intricate and their application to the problem of concern will encounter great difficulty in satisfying the end conditions on the base plane where the stress distribution is of interest.

In the present work, the equations of elasticity for

[*] Graduate student, corresponding author [**] Professor

DOI : 10.1017/jmech.2011.42
Copyright © 2011 The Society of Theoretical and Applied Mechanics, R.O.C.
https://doi.org/10.1017/jmech.2011.42 Published online by Cambridge University Press

axisymmetric deformation of a transversely isotropic body are formulated into a state equation and an output equation in terms of the state vector composed of the displacement and stress variables. The Hamiltonian characteristics of the formulation provide an essential basis for using eigenfunction expansion to determine an exact solution which satisfies the prescribed end conditions..

2. STATE SPACE FORMULATION

Consider a cylinder of a homogeneous material exhibiting transverse anisotropy, as shown in Fig. 1. Suppose the bottom plane is bonded to a rigid base and the top plane of the cylinder is subjected to traction which reduces to a resultant P directed along the axis of the cylinder. Let the origin of the cylindrical coordinates (r, θ, z) be located at the centroid of the fixed section, with the z axis directed along the axis of the cylinder. When the axial force P is the only external force, the deformation and stress fields are independent of θ. On the basis of the state space formalism for the axisymmetric problem in anisotropic elasticity [3], the state equation and the output equation are

$$\frac{\partial}{\partial z}\begin{bmatrix} u_r \\ u_z \\ r\sigma_{rz} \\ r\sigma_{zz} \end{bmatrix} = \begin{bmatrix} 0 & -\partial_r & r^{-1}c_{44}^{-1} & 0 \\ l_{31} & 0 & 0 & r^{-1}c_{33}^{-1} \\ l_{41} & 0 & 0 & l_{46} \\ 0 & 0 & -\partial_r & 0 \end{bmatrix}\begin{bmatrix} u_r \\ u_z \\ r\sigma_{rz} \\ r\sigma_{zz} \end{bmatrix}, \tag{1}$$

$$\begin{bmatrix} r\sigma_{rr} \\ r\sigma_{\theta\theta} \end{bmatrix} = \begin{bmatrix} \tilde{c}_{11}(r\partial_r + 1) - 2c_{66} & \hat{c}_{13} \\ \tilde{c}_{12}(r\partial_r + 1) + 2c_{66} & \hat{c}_{13} \end{bmatrix}\begin{bmatrix} u_r \\ r\sigma_{zz} \end{bmatrix}; \tag{2}$$

where c_{ij} are the elastic constants with reference to the cylindrical coordinates; ∂_r and ∂_z denote partial differentiation with respect to r and z, respectively, and

$$l_{31} = -\hat{c}_{13}(\partial_r + r^{-1}),\ l_{41} = -\tilde{c}_{11}\left[\partial_r(r\partial_r) - r^{-1}\right],$$
$$l_{46} = -\hat{c}_{13}(\partial_r - r^{-1}),\ \tilde{c}_{ij} = c_{ij} - c_{i3}\,c_{33}^{-1}c_{j3},\quad \hat{c}_{ij} = c_{ij}\,c_{33}^{-1}.$$

With $c_{66} = (c_{11} - c_{12})/2$, there are five independent elastic constants for transversely isotropic materials. When the material is isotropic, there are $c_{33} = c_{11}$, $c_{13} = c_{12}$, $c_{44} = c_{66} = (c_{11} - c_{12})/2$.

The cylindrical surface at $r = a$ is traction-free and the upper plane at $c = l$ are subjected to normal tractions,

$$[\sigma_{rr} \quad \sigma_{rz}]_{r=a} = [0 \quad 0],\ [\sigma_{rz} \quad \sigma_{zz}]_{z=l} = \left[0 \quad p(r)\right], \tag{3}$$

with the resultant of normal stress being

$$\int_0^a 2\pi p(r)\,dr = P. \tag{4}$$

The bottom plane is assumed to be perfectly bonded to the rigid base (the fixed end), so the end conditions at $z = 0$ are

$$[u_r \quad u_z]_{z=0} = [0 \quad 0]. \tag{5}$$

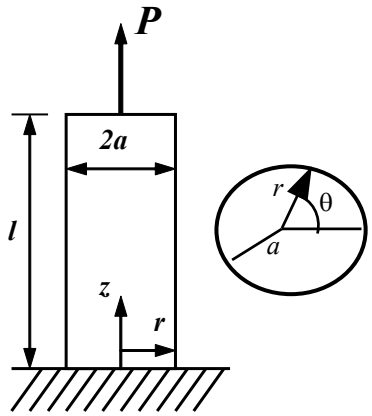


Fig. 1 A circular cylinder subjected to an axial load P

3. SEPERATION OF VARIABLES

We seek the homogeneous solution of Eq. (1) of the form

$$[u_r \quad u_z \quad r\sigma_{rz} \quad r\sigma_{zz}] = [U_r \quad U_z \quad T_{rz} \quad T_{zz}]\,e^{\mu z} \tag{6}$$

where μ is a parameter to be determined; U_r, U_z, T_{rz} and T_{zz} are unknown functions of r, which reduces Eq. (1) to

$$\begin{bmatrix} 0 & -d_r & r^{-1}c_{44}^{-1} & 0 \\ -\hat{c}_{13}(d_r + r^{-1}) & 0 & 0 & r^{-1}c_{33}^{-1} \\ -\tilde{c}_{11}\left[d_r(rd_r) - r^{-1}\right] & 0 & 0 & -\hat{c}_{13}(d_r - r^{-1}) \\ 0 & 0 & -d_r & 0 \end{bmatrix}\begin{bmatrix} U_r \\ U_z \\ T_{rz} \\ T_{zz} \end{bmatrix} = \mu\begin{bmatrix} U_r \\ U_z \\ T_{rz} \\ T_{zz} \end{bmatrix} \tag{7}$$

Equation (7) can be solved by letting

$$\begin{aligned}&[U_r \quad U_r \quad T_{rz} \quad T_{zz}] \\ &= \left[C_1 J_1(\lambda r) \quad C_2 J_0(\lambda r) \quad C_3 r J_1(\lambda r) \quad C_4 r J_0(\lambda r)\right],\end{aligned} \tag{8}$$

where $J_0(\lambda r)$ and $J_1(\lambda r)$ are the Bessel functions of the first kind, of order 0 and 1, respectively; λ and C_j $(i = 1, 2, 3, 4)$ are constants to be determined.

Substituting Eqs. (8) into (7), making use of the derivative formulas:

$$\frac{d}{dr}J_0(\lambda r) = -\lambda J_1(\lambda r),\quad \frac{d}{dr}J_1(\lambda r) = \lambda J_0(\lambda r) - \frac{1}{r}J_1(\lambda r), \tag{9}$$

we arrive at

$$\begin{bmatrix} 0 & \lambda & c_{44}^{-1} & 0 \\ -\hat{c}_{13}\lambda & 0 & 0 & c_{33}^{-1} \\ \tilde{c}_{11}\lambda^2 & 0 & 0 & \hat{c}_{13}\lambda \\ 0 & 0 & -\lambda & 0 \end{bmatrix}\begin{bmatrix} C_1 \\ C_2 \\ C_3 \\ C_4 \end{bmatrix} = \mu\begin{bmatrix} C_1 \\ C_2 \\ C_3 \\ C_4 \end{bmatrix}, \tag{10}$$

https://doi.org/10.1017/jmech.2011.42 Published online by Cambridge University Press

to which non-trivial solutions exist if and only if the determinant of the coefficient matrix equals to zero. This condition yields

$$c_{11}c_{44}\kappa^4 - \left[c_{11}c_{33} - c_{13}(c_{13}+2c_{44})\right]\kappa^2 + c_{33}c_{44} = 0, \quad (\kappa = \lambda/\mu) \tag{11}$$

which has four roots, given by

$$\kappa_1 = -\kappa_3 = \left[\frac{c_{11}c_{33} - c_{13}(c_{13}+2c_{44}) + \sqrt{(c_{11}c_{33}-c_{13}^2)\left[c_{11}c_{33} - (c_{13}+2c_{44})^2\right]}}{2c_{11}c_{44}}\right]^{1/2}$$

$$\kappa_2 = -\kappa_4 = \left[\frac{c_{11}c_{33} - c_{13}(c_{13}+2c_{44}) - \sqrt{(c_{11}c_{33}-c_{13}^2)\left[c_{11}c_{33} - (c_{13}+2c_{44})^2\right]}}{2c_{11}c_{44}}\right]^{1/2}$$

To each $\kappa_j (= \lambda_j / \mu)$ there corresponds a solution of Eq. (10) determined within a constant A_j as

$$\begin{bmatrix} C_1 \\ C_2 \\ C_3 \\ C_4 \end{bmatrix} = A_j \begin{bmatrix} \kappa_j^2 c_{44} - c_{33} \\ \kappa_j (c_{44} + c_{13}) \\ -c_{44}\,\mu(\kappa_j^2 c_{13} + c_{33}) \\ c_{44}\,\mu\kappa_j(\kappa_j^2 c_{13} + c_{33}) \end{bmatrix}, \quad (j = 1, 2, 3, 4) \tag{12}$$

It can be shown on account of positive-definiteness of the stiffness matrix that κ_j (j = 1, 2, 3, 4) cannot be purely imaginary. Since $J_0(-\kappa_j\mu r) = J_0(\kappa_j\mu r)$ and $J_1(-\kappa_j\mu r) = -J_1(\kappa_j\mu r)$, there are two linearly independent solutions derivable from Eqs. (8) ~ (12). The complete solution of Eqs. (1) ~ (2) is

$$\begin{bmatrix} u_r \\ u_z \\ r\sigma_{rz} \\ r\sigma_{zz} \end{bmatrix} = \sum_{j=1}^{2} A_j\, e^{\mu z} \begin{bmatrix} f_1(\kappa_j, \mu, r) \\ f_2(\kappa_j, \mu, r) \\ f_3(\kappa_j, \mu, r) \\ f_4(\kappa_j, \mu, r) \end{bmatrix}, \tag{13}$$

$$\begin{bmatrix} r\sigma_{rr} \\ r\sigma_{\theta\theta} \end{bmatrix} = \sum_{j=1}^{2} A_j\, e^{\mu z} \begin{bmatrix} f_5(\kappa_j, \mu, r) \\ f_6(\kappa_j, \mu, r) \end{bmatrix}, \tag{14}$$

where

$$\begin{bmatrix} f_1(\kappa_j, \mu, r) \\ f_2(\kappa_j, \mu, r) \\ f_3(\kappa_j, \mu, r) \\ f_4(\kappa_j, \mu, r) \end{bmatrix} = \begin{bmatrix} (\kappa_j^2 c_{44} - c_{33}) J_1(\kappa_j \mu r) \\ \kappa_j (c_{44} + c_{13}) J_0(\kappa_j \mu r) \\ -c_{44}\,\mu(\kappa_j^2 c_{13} + c_{33}) r J_1(\kappa_j \mu r) \\ c_{44}\,\mu(\kappa_j^2 c_{13} + c_{33}) r J_0(\kappa_j \mu r) \end{bmatrix},$$

$$f_5(\kappa_j, \mu, r) = \left[c_{44}(\kappa_j^2 c_{11} + c_{13}) - \tilde{c}_{11} c_{33}\right] \kappa_j \mu r J_0(\kappa_j \mu r) - 2c_{66}(\kappa_j^2 c_{44} - c_{33}) J_1(\kappa_j \mu r),$$

$$f_6(\kappa_j, \mu, r) = \left[c_{44}(\kappa_j^2 c_{12} + c_{13}) - \tilde{c}_{12} c_{33}\right] \kappa_j \mu r J_0(\kappa_j \mu r) + 2_{C66}(\kappa_j^2 c_{44} - c_{33}) J_1(\kappa_j \mu r).$$

In case of isotropy, Eq. (11) yield $\kappa_1 = \kappa_2 = 1$ and $\kappa_3 = \kappa_4 = -1$, which are repeated. Thus, only one eigenvector is obtained by substituting $\kappa = \pm 1$ in Eqs. (13) ~ (14). Since a linear combination of the eigenvectors for $\kappa_2 \neq \kappa_1$ is also an eigenvector of a linear system, the other one linearly independent eigenvector is determined through a limiting process by letting $\kappa_2 \to \kappa_1 = 1$ and $\kappa_4 \to \kappa_3 = -1$. A linear combination of these two linearly independent eigenvectors together gives the solution of Eqs. (1) ~ (2) for isotropic materials [4].

4. SATISFACTION OF THE BOUNDARY CONDITIONS

Imposing Eq. (3) on Eqs. (13) ~ (14) gives

$$\begin{bmatrix} f_3(\kappa_1, \mu, a) & f_3(\kappa_2, \mu, a) \\ f_5(\kappa_1, \mu, a) & f_5(\kappa_2, \mu, a) \end{bmatrix} \begin{bmatrix} A_1 \\ A_2 \end{bmatrix} = \begin{bmatrix} 0 \\ 0 \end{bmatrix}. \tag{15}$$

Nontrivial solution of Eq. (15) exists if and only if the determinant of the coefficient matrix is zero. This condition leads to a transcendental equation

$$\eta_1 J_1(\kappa_1 \mu a) J_1(\kappa_2 \mu a) + \mu a \left[\eta_2 J_1(\kappa_1 \mu a) J_0(\kappa_2 \mu a) - \eta_3 J_0(\kappa_1 \mu a) J_1(\kappa_2 \mu a)\right] = 0, \tag{16}$$

where

$$\eta_1 = 2c_{66}\, c_{33}(c_{13} + c_{44})(\kappa_1^2 - \kappa_2^2),$$

$$\eta_2 = \kappa_2(\kappa_1^2 c_{13} + c_{33})[\kappa_2^2 c_{44} c_{11} + c_{13}(c_{44} + c_{13}) - c_{11} c_{33}],$$

$$\eta_3 = \kappa_1(\kappa_2^2 c_{13} + c_{33})[\kappa_1^2 c_{44} c_{11} + c_{13}(c_{44} + c_{13}) - c_{11} c_{33}].$$

By inspection, if μ is a root of Eq. (16), so is $-\mu$. Moreover, $\mu = 0$ is a repeated root, which can be verified by replacing μ by $-\mu$ in Eq. (16) and using the fact that $\mu = 0$ is a zero of $J_1(\kappa\mu a)$ and $J_0(-\kappa_j\mu r) = J_0(\kappa_j\mu r)$, $J_1(-\kappa_j\mu r) = -J_1(\kappa_j\mu r)$.

Substituting the eigenvalues μ_i (i = 1, 2, …) determined from Eq. (16) back to Eq. (15), expressing A_{2i} in terms of A_{1i}, we obtain

$$A_{2i} = -\frac{f_3(\kappa_1, \mu_i, a)}{f_3(\kappa_2, \mu_i, a)} A_{1i} \equiv a_i\, A_i, \tag{17}$$

The case of $\mu_0 = 0$ requires special consideration. Since $\mu_0 = 0$ is a repeated root of Eq. (16), only one of the eigenvectors associated with $\mu_0 = 0$ is obtained from Eqs. (15) ~ (17):

$$\begin{aligned} &[u_r \quad u_z \quad r\sigma_{rz} \quad r\sigma_{zz}] = [0 \quad 1 \quad 0 \quad 0], \\ &[r\sigma_{rr} \quad r\sigma_{\theta\theta}] = [0 \quad 0], \end{aligned} \tag{18}$$

which is a rigid body translation in z axis.

Another linearly independent eigenvector associated with $\mu_0 = 0$ can be determined by considering the Jordan-chain solution [4] as

$$\begin{aligned} &[u_r \quad u_z \quad r\sigma_{rz} \quad r\sigma_{zz}] = [\beta_1 r \quad z \quad 0 \quad \beta_2 r], \\ &[r\sigma_{rr} \quad r\sigma_{\theta\theta}] = [0 \quad 0], \end{aligned} \tag{19}$$

https://doi.org/10.1017/jmech.2011.42 Published online by Cambridge University Press

where

$$\beta_1 = -\frac{c_{13}}{c_{11}+c_{12}}, \quad \beta_2 = \frac{c_{33}(c_{11}+c_{12})-2c_{13}^2}{c_{11}+c_{12}},$$

A linear combination of the eigensolutions produces the complete solution of Eqs. (1) ~ (2):

$$\begin{bmatrix} u_r \\ u_z \\ r\sigma_{rz} \\ r\sigma_{zz} \end{bmatrix} = A_0 \begin{bmatrix} 0 \\ 1 \\ 0 \\ 0 \end{bmatrix} + B_0 \begin{bmatrix} \beta_r\, r \\ z \\ 0 \\ \beta_2\, r \end{bmatrix} + \sum_{i=1}^{\infty} \left(A_i\, e^{\mu_i z} \begin{bmatrix} h_1(\mu_i, r) \\ h_2(\mu_i, r) \\ h_3(\mu_i, r) \\ h_4(\mu_i, r) \end{bmatrix} + A_{-i}\, e^{-\mu_i z} \begin{bmatrix} h_1(-\mu_i, r) \\ h_2(-\mu_i, r) \\ h_3(-\mu_i, r) \\ h_4(-\mu_i, r) \end{bmatrix} \right) \tag{20}$$

$$\begin{bmatrix} r\sigma_{rr} \\ r\sigma_{rr} \end{bmatrix} = \sum_{i=1}^{\infty} \left(A_i\, e^{\mu_i z} \begin{bmatrix} h_5(\mu_i, r) \\ h_6(\mu_i, r) \end{bmatrix} + A_{-i}\, e^{-\mu_i z} \begin{bmatrix} h_5(-\mu_i, r) \\ h_6(-\mu_i, r) \end{bmatrix} \right), \tag{21}$$

where A_0, B_0, A_i and A_{-i} are constants of linear combination, and

$$h_j(\mu_i, r) = f_j(\kappa_1, \mu_i, r) + \alpha f_j(\kappa_2, \mu_i, r), \quad (j = 1, 2, \cdots, 6).$$

5. SATISFACTION OF THE END CONDITIONS

The solution is required to satisfy the end conditions at $z = 0$ and $z = l$. To this end, imposing Eqs. (4) ~ (5) on Eq. (20), we obtain for the case of fixed end at $z = 0$ and free end at $z = l$:

$$\mathbf{F}_0(r) = \sum_{i=0}^{\infty} \left[A_i\, \boldsymbol{\psi}_i(r) + A_{-i}\, \boldsymbol{\psi}_{-i}(r) \right] + A_0\, \boldsymbol{\psi}_0^{(0)} + B_0\, \boldsymbol{\psi}_0^{(1)}(r), \tag{22}$$

$$\mathbf{F}_l(r) = \sum_{i=0}^{\infty} \left[A_i\, e^{\mu_i l} \boldsymbol{\psi}_i(r) + A_{-i}\, e^{-\mu_i l} \boldsymbol{\psi}_{-i}(r) \right] + (A_0 + B_0\, l) \boldsymbol{\psi}_0^{(0)} + B_0\, \boldsymbol{\psi}_0^{(1)}(r), \tag{23}$$

where

$$\boldsymbol{\psi}_i(r) = \begin{bmatrix} h_1(\mu_i, r) \\ h_2(\mu_i, r) \\ h_3(\mu_i, r) \\ h_4(\mu_i, r) \end{bmatrix}, \boldsymbol{\psi}_{-i}(r) = \begin{bmatrix} h_1(-\mu_i, r) \\ h_2(-\mu_i, r) \\ h_3(-\mu_i, r) \\ h_4(-\mu_i, r) \end{bmatrix}, \quad \boldsymbol{\psi}_0^{(0)} = \begin{bmatrix} 0 \\ 1 \\ 0 \\ 0 \end{bmatrix},$$

$$\boldsymbol{\psi}_0^{(1)}(r) = \begin{bmatrix} \beta_1\, r \\ 0 \\ 0 \\ \beta_2\, r \end{bmatrix}, \quad \mathbf{F}_0(r) = \begin{bmatrix} 0 \\ 0 \\ r\sigma_{rz}(r, 0) \\ r\sigma_{zz}(r, 0) \end{bmatrix}, \quad \mathbf{F}_l(r) = \begin{bmatrix} u_r(r, l) \\ u_z(r, l) \\ 0 \\ p(r) \end{bmatrix},$$

in which A_0, B_0, A_i and A_{-i} are constants to be determined, $\mathbf{F}_0(r)$ contains the unknown tractions $\sigma_{rz}(r, 0)$ and $\sigma_{zz}(r, 0)$ at the fixed end, $\mathbf{F}_l(r)$ contains the unknown displacements $u_r(r, l)$ and $u_z(r, l)$ at the free end, which, in turn, can be expressed in terms of A_0, B_0, A_i and A_{-i} by using Eqs. (13) ~ (14) as

$$r\sigma_{rz}(r, 0) = \sum_{i=1}^{\infty} \left[A_i\, h_3(\mu_i, r) + A_{-i}\, h_3(-\mu_i, r) \right], \tag{24}$$

$$r\sigma_{zz}(r, 0) = \sum_{i=1}^{\infty} \left[A_i\, h_4(\mu_i, r) + A_{-i}\, h_4(-\mu_i, r) \right] + B_0\, \beta_2\, r, \tag{25}$$

$$u_r(r, l) = \sum_{i=1}^{\infty} \left[A_i\, e^{\mu_i l} h_1(\mu_i, r) + A_{-i}\, e^{-\mu_i l} h_1(-\mu_i, r) \right] + B_0\, \beta_1\, r, \tag{26}$$

$$u_z(r, l) = \sum_{i=1}^{\infty} \left[A_i\, e^{\mu_i l} h_2(\mu_i, r) + A_{-i}\, e^{-\mu_i l} h_2(-\mu_i, r) \right] + A_0 + B_0\, l. \tag{27}$$

At this stage, it remains to determine the constants A_0, B_0, A_i and A_{-i} in Eqs. (22) ~ (23). For this purpose, the symplectic orthogonality relations of the eigenvectors is to be used to express a given vector function in terms of the eigenvectors via eigenfunction expansion.

6. SYMPLECTIC ORTHOGONALITY

While the characteristics of certain constant system matrices, such as a real symmetric matrix or a Hermitian matrix, are well known [5], the characteristics of a Hamiltonian system matrix [6] are less recognized, particularly when the matrix involves differential operators. Tarn *et al*. [4] delineated the Hamiltonian characteristics of the formulation and symplectic orthogonality of the eigenvectors for axisymmetric deformations.

To facilitate exposition, let us express Eq. (7) with the homogeneous BC at $r = 0$ and $r = a$ as

$$\mathbf{H}\boldsymbol{\psi} = \mu\boldsymbol{\psi}, \quad \mathbf{B}(\boldsymbol{\psi}) = \mathbf{0}, \tag{28}$$

where

$$\mathbf{H} = \begin{bmatrix} \mathbf{L}_{11} & \mathbf{L}_{12} \\ \mathbf{L}_{21} & -\mathbf{L}_{11} \end{bmatrix}, \quad \boldsymbol{\psi} = \begin{bmatrix} \mathbf{u} \\ \boldsymbol{\tau} \end{bmatrix}, \quad \mathbf{u} = \begin{bmatrix} U_r \\ U_z \end{bmatrix}, \quad \boldsymbol{\tau} = \begin{bmatrix} T_{rz} \\ T_{zz} \end{bmatrix},$$

$$\mathbf{L}_{11} = \begin{bmatrix} 0 & -d_r \\ -\hat{c}_{13}(d_r + r^{-1}) & 0 \end{bmatrix}, \quad \mathbf{L}_{12} = \begin{bmatrix} r^{-1}c_{44}^{-1} & 0 \\ 0 & r^{-1}c_{33}^{-1} \end{bmatrix},$$

$$\mathbf{L}_{11}^* = \begin{bmatrix} 0 & \hat{c}_{13}(d_r - r^{-1}) \\ d_r & 0 \end{bmatrix}, \quad \mathbf{L}_{21} = \begin{bmatrix} -\tilde{c}_{11}\left[d_r(rd_r) - r^{-1} \right] & 0 \\ 0 & 0 \end{bmatrix}.$$

The matrix $\mathbf{H}$ in Eq. (28) exhibits the characteristics of a Hamiltonian matrix such that $\mathbf{L}_{12}$ and $\mathbf{L}_{21}$ are symmetric matrix and the operators $\mathbf{L}_{11}$ and $\mathbf{L}_{11}^*$ are adjoint. Such characteristics are of fundamental significance in the formulation.

https://doi.org/10.1017/jmech.2011.42 Published online by Cambridge University Press

First of all, the adjoint system of Eq. (28) [4] is

$$\mathbf{H}\boldsymbol{\varphi} = -\mu\boldsymbol{\varphi}\,, \quad \mathbf{B}(\boldsymbol{\varphi}) = \mathbf{0}\,, \tag{29}$$

where $\boldsymbol{\varphi}$ is the eigenvector associated with the eigenvalue $-\mu$,

$$\boldsymbol{\varphi} = \begin{bmatrix} \mathbf{v} \\ \mathbf{s} \end{bmatrix}, \quad \mathbf{v} = \begin{bmatrix} V_r \\ V_z \end{bmatrix}, \quad \mathbf{s} = \begin{bmatrix} S_{rz} \\ S_{zz} \end{bmatrix}.$$

Equations (28) and (29) reveal that if μ is an eigenvalue of $\mathbf{H}$, so is $-\mu$. It follows that $\mu = 0$ must be a repeated eigenvalue. Indeed, the eigenvalues determined from Eq. (16) verify this important property of an axisymmetric Hamiltonian system.

Consider two linearly independent eigenvectors ψ_i and ψ_j associated with the eigenvalues μ_i and μ_j, respectively,

$$\mathbf{H}\boldsymbol{\psi}_i = \mu_i\,\boldsymbol{\psi}_i\,, \quad \mathbf{B}(\boldsymbol{\psi}_i) = \mathbf{0}\,, \tag{30}$$

$$\mathbf{H}\boldsymbol{\psi}_j = \mu_j\,\boldsymbol{\psi}_j\,, \quad \mathbf{B}(\boldsymbol{\psi}_j) = \mathbf{0}\,. \tag{31}$$

There follows the symplectic orthogonal relation for the eigenvectors associated with $\mu_i \neq 0$ ($i = 1, 2, \ldots$) [4]:

$$\int_0^a \boldsymbol{\psi}_i^T \mathbf{J}\boldsymbol{\psi}_j\, dr = \begin{cases} = 0\,, & (j \neq -i) \\ \neq 0\,, & (j = -i) \end{cases} \tag{32}$$

The case of the repeated eigenvalue $\mu_0 = 0$ needs special consideration. The two linearly independent eigenvectors $\boldsymbol{\psi}_0^{(1)}$ and $\boldsymbol{\psi}_0^{(2)}$ can be determined from the Jordan chain associated with $\mu_0 = 0$:

$$\mathbf{H}\boldsymbol{\psi}_0^{(0)} = \mathbf{0}\,, \quad \mathbf{B}(\boldsymbol{\psi}_0^{(0)}) = \mathbf{0}\,, \tag{33}$$

$$\mathbf{H}\boldsymbol{\psi}_0^{(1)} = \boldsymbol{\psi}_0^{(0)}, \quad \mathbf{B}(\boldsymbol{\psi}_0^{(1)}) = \mathbf{0}\,. \tag{34}$$

from which we obtain

$$\boldsymbol{\psi}_0^{(1)} = \boldsymbol{\psi}_0^{(0)} = [0 \;\; 1 \;\; 0 \;\; 0]^T\,, \tag{35}$$

$$\boldsymbol{\psi}_0^{(2)} = \boldsymbol{\psi}_0^{(1)} + z\boldsymbol{\psi}_0^{(0)} = [\beta_1\, r \;\; 0 \;\; 0 \;\; \beta_2\, r]^T + z[0 \;\; 1 \;\; 0 \;\; 0]^T\,. \tag{36}$$

The symplectic orthogonal relations of the eigenvectors associated with $\mu_0 = 0$ [4] are

$$\int_0^a (\boldsymbol{\psi}_0^{(\alpha)})^T \mathbf{J}\boldsymbol{\psi}_0^{(\beta)} dr \begin{cases} = 0\,, & (\beta = \alpha\;;\alpha, \beta = 0, 1) \\ \neq 0\,, & (\beta \neq \alpha\;;\;\alpha, \beta = 0, 1) \end{cases} \tag{37}$$

Symplectic orthogonality in the present formulation holds for the eigenvectors in the Hamiltonian state space, with which it is possible to express an arbitrary integrable state vector in terms of a sequence of orthogonal eigenvectors by means of eigenfunction expansion.

7. DETERMINING THE UNKNOWN CONSTANTS

Returning to the task of determining A_0, B_0, A_i and A_{-i} in Eqs. (22) and (23). Let us consider the case of the fixed end at $z = 0$ in detail.

Multiplying both sides of Eq. (22) by $\boldsymbol{\psi}_{-i}^T\mathbf{J}$, $\boldsymbol{\psi}_i^T\mathbf{J}$, $[\boldsymbol{\psi}_0^{(1)}]^T\mathbf{J}$, and $[\boldsymbol{\psi}_0^{(1)}]^T\mathbf{J}$, respectively, and integrating them over (0, a), making use of the symplectic orthogonality in Eqs. (32) and (37), we obtain

$$A_i = \int_0^a \boldsymbol{\psi}(r)\mathbf{J}\mathbf{F}_0(r)\, dr\,, \quad A_{-i} = -\int_0^a \boldsymbol{\psi}_i^T(r)\mathbf{J}\mathbf{F}_0(r)\, dr\,, \tag{38}$$

$$A_0 = \int_0^a \left[\boldsymbol{\psi}_0^{(1)}(r)\right]^T \mathbf{J}\mathbf{F}_0(r)\, dr\,,$$
$$B_0 = -\int_0^a \left[\boldsymbol{\psi}_0^{(0)}(r)\right]^T \mathbf{J}\mathbf{F}_0(r)\, dr\,, \tag{39}$$

Likewise, there follow from Eq. (23)

$$A_i = e^{-\mu l}\int_0^a \boldsymbol{\psi}_{-i}^T(r)\mathbf{J}\mathbf{F}_l(r)\, dr\,,$$
$$A_{-i} = -e^{-\mu l}\int_0^a \boldsymbol{\psi}_i^T(r)\mathbf{J}\mathbf{F}_l(r)\, dr\,, \tag{40}$$

$$A_0 + B_0\, l = \int_0^a \left[\boldsymbol{\psi}_0^{(1)}(r)\right]^T \mathbf{J}\mathbf{F}_l(r)\, dr\,,$$
$$B_0 = -\int_0^a \left[\boldsymbol{\psi}_0^{(0)}(r)\right]^T \mathbf{J}\mathbf{F}_l(r)\, dr\,, \tag{41}$$

In Eqs. (38) ~ (41) the vectors $\mathbf{F}_0(r)$ and $\mathbf{F}_l(r)$ contain four components each, of which the tractions $\sigma_{rz}(r, 0)$ and $\sigma_{zz}(r, 0)$ are unknowns at the fixed end $z = 0$, the displacements $u_r(r, l)$ and $u_z(r, l)$ are unknowns at the free end $z = l$. Substituting Eqs. (38) ~ (39) in Eqs. (40) ~ (41) gives

$$\int_0^a \boldsymbol{\psi}_{-i}^T(r)\mathbf{J}\left[\mathbf{F}_0(r) - e^{-\mu l}\mathbf{F}_l(r)\right] dr = 0\,, \tag{42}$$

$$\int_0^a \boldsymbol{\psi}_i^T(r)\mathbf{J}\left[\mathbf{F}_0(r) - e^{-\mu l}\mathbf{F}_l(r)\right] dr = 0\,, \tag{43}$$

$$\int_0^a \left\{\left[\boldsymbol{\psi}_0^{(1)}(r)\right]^T \mathbf{J}\left[\mathbf{F}_0(r) - \mathbf{F}_l(r)\right] - l\left[\boldsymbol{\psi}_0^{(0)}(r)\right]^T \mathbf{J}\mathbf{F}_0(r)\right\} dr = 0\,, \tag{44}$$

$$\int_0^a \left[\boldsymbol{\psi}_0^{(0)}(r)\right]^T \mathbf{J}\left[\mathbf{F}_0(r) - \mathbf{F}_l(r)\right] dr = 0\,, \tag{45}$$

in which the four unknown functions in $\mathbf{F}_0(r)$ and $\mathbf{F}_l(r)$ are related to the constants A_0, B_0, A_i and A_{-i} through Eqs. (24) ~ (27).

Substituting Eqs. (24) ~ (27) in Eqs. (42) ~ (45) and taking N terms of the series for computation, we arrive at a system of $2N + 2$ algebraic equations for the $2N + 2$ unknowns: A_0, B_0, A_i and A_{-i} ($i = 1, 2, \ldots, N$) which can be solved by using a standard method.

https://doi.org/10.1017/jmech.2011.42 Published online by Cambridge University Press

8. THE SAINT-VENANT SOLUTION

By assuming a uniaxial stress state and disregarding the boundary conditions on the base plane, the Saint-Venant solution [2] satisfies the equations of anisotropic elasticity, the uniform traction BC with the average value $\sigma_0 = P/A$ on the top plane and the traction-free BC on the lateral surface of the cylinder:

$$[u_r \quad u_z \quad r\sigma_{rz} \quad r\sigma_{zz}] = \sigma_0[a_{13}\, r \quad a_{33}\, z \quad 0 \quad r], \tag{46}$$

$$[r\sigma_{rr} \quad r\sigma_{\theta\theta}] = [0 \quad 0], \tag{47}$$

where A is the cross section area πa^2; the elastic compliances a_{ij} are related to the elastic constants c_{ij} by

$$a_{13} = c_{13}(c_{12} - c_{11})/\Delta, \quad a_{33} = (c_{11}^2 - c_{12}^2)/\Delta,$$
$$\Delta = \begin{vmatrix} c_{11} & c_{12} & c_{13} \\ c_{12} & c_{11} & c_{13} \\ c_{13} & c_{13} & c_{33} \end{vmatrix}.$$

The solution is valid provided that the base plane is free to distort in compliance with the assumed uniaxial stress state. Yet, in reality, the base plane of the cylinder is not free to distort and the end conditions are prescribed rather than assigned a posterior.

9. RESULTS AND DISCUSSIONS

To evaluate the end effects on the deformation and stress distribution in the cylinder, the results are compared with the corresponding ones according to the Saint-Venant solution in Eqs. (46) ~ (47). The results obtained depend upon the material and the size of the cylinder. For numerical calculations using MATLAB, the following dimensionless elastic constants for isotropic and transversely isotropic materials are taken: $c_{33} / c_{11} = 1$, 5, 10, 20; $c_{12} / c_{11} = c_{13} / c_{11} = 1/3$. The dimensionless length of the cylinder is taken to be $l/a = 10$.

Table 1 shows the first 25 dimensionless quantities μa associated with the eigenvalues for the material parameters considered, in which the eigenvalues are found from Eq. (16). The first eigenvalue in all cases is zero and it is a repeated eigenvalue, with which associated linearly z-dependent displacements and z-independent stresses. The non-zero eigenvalues are related to the stress disturbance by the end conditions. All the eigenvalues for the isotropic material are complex conjugate, and the eigenvalues for transversely isotropic materials are mostly real. Variations of the displacements and stresses in the cylinders are evaluated by taking N terms in the eigenfunction expansion. The number N can be chosen as large as necessary to achieve a required accuracy. Due to significant end effect, displacement and stress results in region near the ends converge rather slowly (requiring up to 40 terms). In region away from the ends, the results converge rapidly (requiring less than 20 terms).

Table 1 The dimensionless eigenvalues (μa) for isotropic and transversely isotropic materials ($c_{12} / c_{11} = c_{13} / c_{11} = 1/3$)

mode	$c_{33}/c_{11}=1$ (isotropic)	$c_{33}/c_{11}=5$	$c_{33}/c_{11}=10$	$c_{33}/c_{11}=20$
1	0	0	0	0
2	2.698±1.367i	1.061	0.723	0.503
3	6.051±1.638i	1.955	1.324	0.920
4	9.261±1.829i	2.921	1.924	1.335
5	12.438±1.967i	3.456±0.363i	2.532	1.749
6	15.602±2.076i	4.378	3.204	2.164
7	18.760±2.166i	5.282	3.535±0.241i	2.583
8	21.912±2.242i	6.160	4.194	3.011
9	25.062±2.308i	7.036	4.812	3.514±0.149i
10	28.210±2.367i	7.933	5.412	3.678
11	31.358±2.419i	8.851±0.311i	6.008	4.171
12	34.504±2.466i	9.442	6.602	4.595
13	37.649±2.510i	10.382	7.197	5.012
14	40.794±2.549i	11.263	7.796	5.426
15	43.939±2.586i	12.138	8.407	5.840
16	47.083±2.621i	13.027	9.082±0.195i	6.253
17	50.227±2.653i	14.075±0.236i	9.429	6.665
18	53.370±2.683i	14.489	10.089	7.078
19	56.514±2.712i	15.482	10.693	7.491
20	59.657±2.738i	16.365	11.290	7.906
21	62.800±2.764i	17.240	11.884	8.323
22	65.943±2.788i	18.125	12.479	8.750
23	69.086±2.812i	19.199	13.076	9.208±0.141i
24	72.228±2.834i	19.444±0.146i	13.683	9.466
25	75.371±2.855i	20.582	14.471±0.094i	9.922

Figure 2 depicts variations of u_r, u_z, σ_{rr} and $\sigma_{\theta\theta}$ around the rim ($r = a$) (where $\sigma_{rz} = \sigma_{rr} = 0$) in the axial direction within a diameter from the fixed end. The dot lines in the figure are the results given by the Saint-Venant solution, Eqs. (46) ~ (47), which obtains an uniform stress distribution and allow the cylinder to freely expand laterally, except at the fixed end ($z = 0$). The points at $r = a$ are around the rim of the cylinder where the results significantly different from the Saint-Venant ones are to be expected. Indeed, remarkable differences of u_r, σ_{zz} and $\sigma_{\theta\theta}$ from those of the Saint-Venant solution exist in the region within a distance of the cylinder diameter near the fixed end. The fixed end effects diminish rapidly. At a distance of a diameter from the base plane, the Saint-Venant solution produces essentially the same results as those obtained from the present analysis. This implies that the end effect is confined to a local region near the fixed end for cylinders of typical engineering materials under the extension. Since the base plane of a fiber-reinforced cylinder under the extension experiences smaller axial deformation than the one without fiber reinforcements, consequently, as the axial stiffness increases, the end effect on the stress field decreases and the stress state tends to be uniaxial.

Figures 3 and 4 depict variations of displacements and stresses in the radial direction at $z = 0.1a$ and at the fixed end $z = 0$. The lateral BC $\sigma_{rz} = \sigma_{rr} = 0$ at $r = a$ are satisfied as required. The stresses σ_{rr}, $\sigma_{\theta\theta}$ and σ_{rz} are small but nonzero, whereas the Saint-Venant solution gives $\sigma_{rr} = \sigma_{\theta\theta} = \sigma_{rz} = 0$. Remarkable differences

https://doi.org/10.1017/jmech.2011.42 Published online by Cambridge University Press

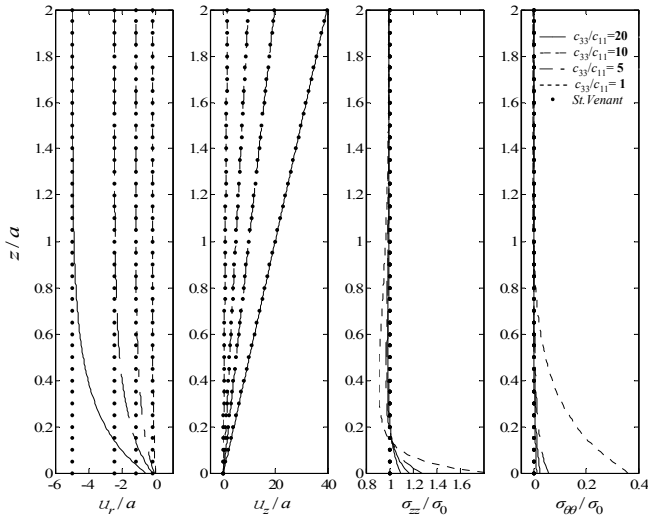


Fig. 2 Axial variations of displacements and stresses in $z = 0 \sim 2a$ at the rim ($r = a$) of the cylinder with a fixed end

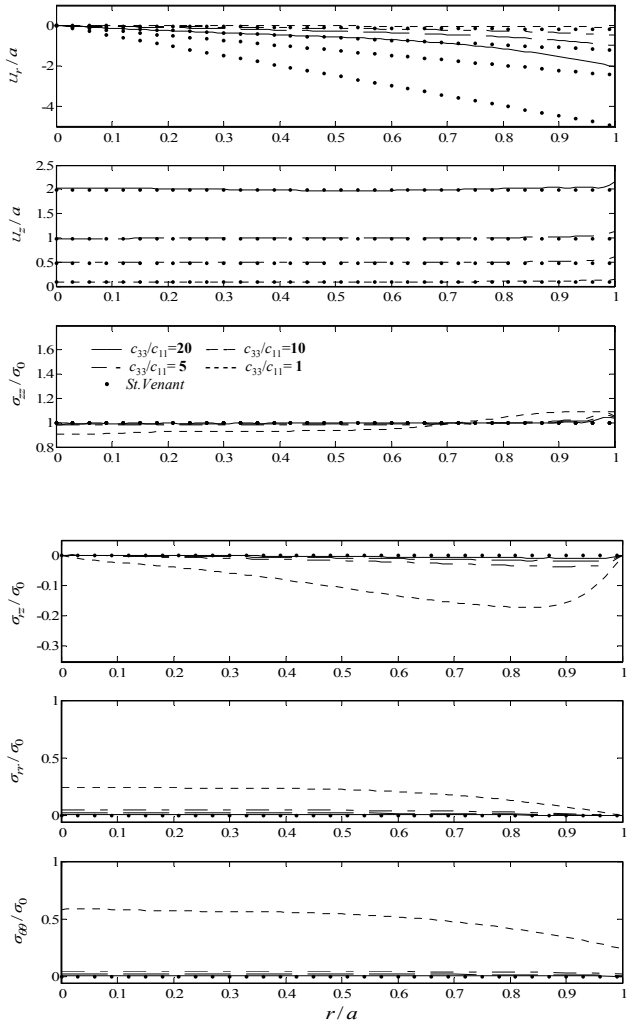


Fig. 3 Radial variations of displacements and stresses at $z = 0.1a$, with fixed end at $z = 0$

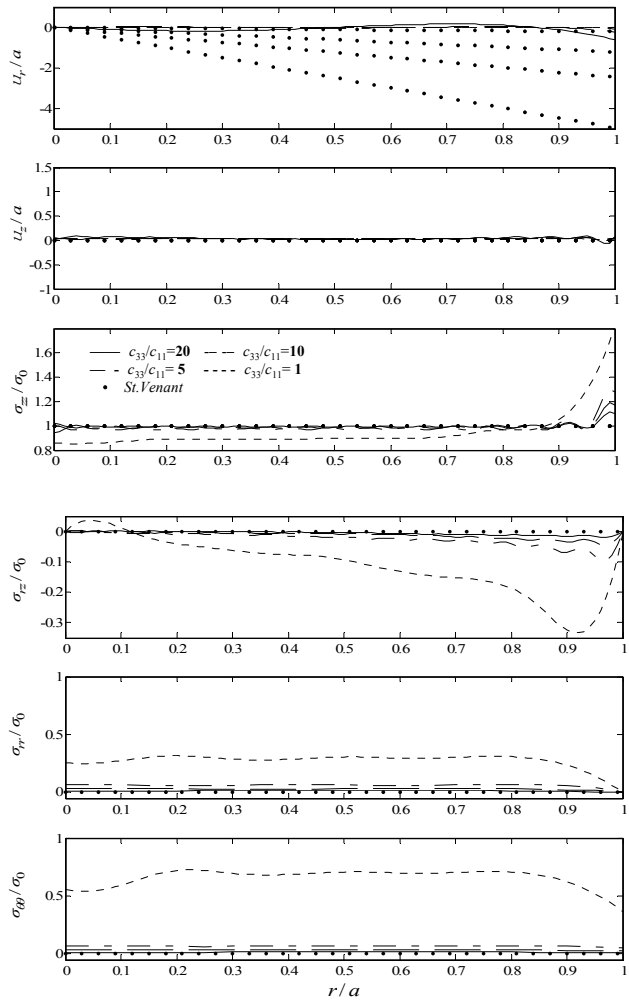


Fig. 4 Radial variations of displacements and stresses at fixed end ($z = 0$)

in the axial stress σ_{zz} from the one given by the Saint-Venant solution exist around the rim of the cylinder. This is expected because the fixed end conditions $u_r = u_z = 0$ at $z = 0$ are not satisfied by the Saint-Venant solution. Figure 4 shows that the lateral BC and end conditions are satisfied in the present analysis. Obviously, the Saint-Venant solution assuming a uniaxial stress state fails to provide valid deformation and stress distribution at least on the base of the cylinder where the stress concentration near the rim is expected to occur. It should be noted that, when the end condition on the base plane involves displacements (as it usually does), the end effects cannot be dismissed on the ground of Saint-Venant's principle. The stresses σ_{zz} and σ_{rz} overshoot near the boundary points at $r = a$, indicating stress concentration appears at the rim on the base plane at the fixed end due to geometric discontinuity. For isotropic materials, the values of σ_{zz} and σ_{rz} near $r = a$ reach $1.8\sigma_0$ and $0.34\sigma_0$, respectively, comparing with $\sigma_{zz} = \sigma_0$ and $\sigma_{rz} = 0$ according to the Saint-Venant solution. As a consequence of the series solution using eigenfunction expansion, the axial stress σ_{zz} and the shear stress σ_{rz} at the base plane are oscillating with respect to mean values. Since all the eigenvalues for the isotropic material are complex conjugate, sug-

https://doi.org/10.1017/jmech.2011.42 Published online by Cambridge University Press

gesting that the series solution will yield results oscillating more in the case of isotropy than in the case of transverse isotropy. This is reflected in the figure. It reduces rapidly at a distance $z = 0.1a$ away from the fixed end.

To show the effect of the concentrated load applied at the end ($z = 10a$) of a slender cylinder, Fig. 5 depicts axial variations of u_z, σ_{zz}, σ_{rr} and $\sigma_{\theta\theta}$ at the centroid ($r = 0$; where $u_r = 0$, $\sigma_{rz} = 0$) in the region ($z = 5a \sim 9.5a$) where the end effect is significant to be expected. It is quite noticeable that high localized displacements and stresses occur within at least a distance of the cylinder diameter near the end. The concentration is smaller and the stress state tends to be uniaxial in the points farer away from the end. Since the plane of a fiber-reinforced cylinder under the extension can resist higher localized axial deformation than the one without fiber reinforcements, consequently, as the axial stiffness increases, the axial effects of u_z and σ_{zz} increase (the in-plane effects of σ_{rr} and $\sigma_{\theta\theta}$ decrease) but diminish more rapidly.

Figures 6 and 7 depict the radial variations of displacements and stresses over cross sections at $z = 9.9a$ and at $z = 9.5a$ in the vicinity of the point of application of the load, where the Saint-Venant solution fails to provide valid non-uniform distribution. In Fig. 6, we observe that remarkable differences in u_z and σ_{zz} from the one given by the Saint-Venant solution exist around the centroid of the cylinder. The lateral BC $\sigma_{rz} = \sigma_{rr} = 0$ at $r = a$ are satisfied as required. The stresses σ_{rr}, $\sigma_{\theta\theta}$ and σ_{rz} are small but nonzero, whereas the Saint-Venant solution gives $\sigma_{rr} = \sigma_{\theta\theta} = \sigma_{rz} = 0$. As we move away from the end, the distribution gradually approaches the uniform as shown in Fig. 7.

Figure 8 shows the result of the radial distribution of normal stress σ_{zz} across various sections ($z = 8a$, $9a$, $9.5a$) of a cylinder made of isotropic material and subjected to the concentrated load. Defines the ratio of the maximum value of σ_{zz} over the average value σ_0 in the critical sections as the stress-concentration factor σ_{zz} / σ_0. The stress-concentration factor reaches 5.15 at $z = 9.5a$ and reduces to 1.6 at $z = 9a$, comparing with $\sigma_{zz} / \sigma_0 = 1$ according to the Saint-Venant solution. As we consider elements farther and farther from the end ($z \le 8a$), we note a progressive equalization of the deformations involved, and thus a more nearly uniform distribution of the stresses across a section of the cylinder. It is evident that at a distance from the end equal to diameter ($2a$) of the cylinder the stress distribution is practically uniform, which confirms the conclusion usually made on the basis of Saint-Venant's principle.

10. CONCLUSIONS

On the basis of Hamiltonian state space formulation, an exact analysis of the deformations and stress distributions in the cylinders of transversely isotropic and isotropic elastic materials is conducted. The results

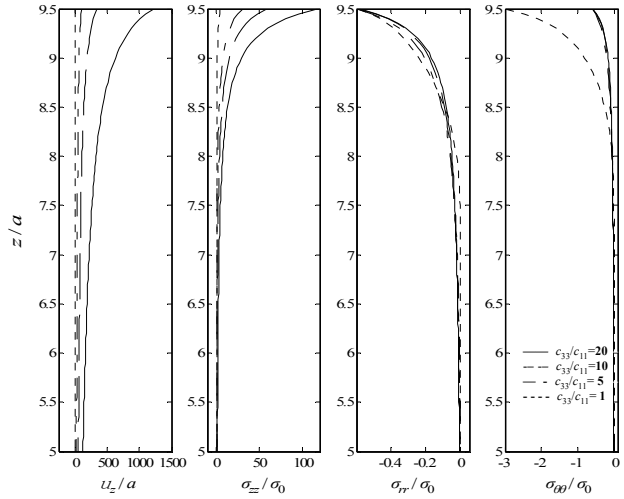


Fig. 5 Axial variations of displacements and stresses in $z = 5a \sim 9.5a$ at the centroid ($r = 0$) of the cylinder subjected to P

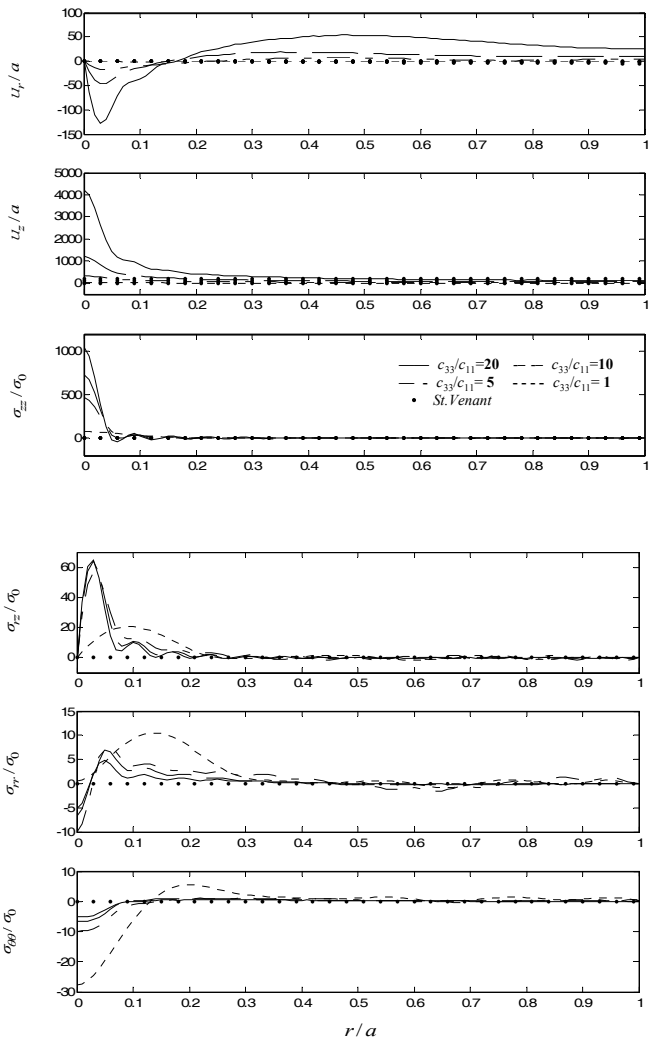


Fig. 6 Radial variations of displacements and stresses at $z = 9.9a$, under P

https://doi.org/10.1017/jmech.2011.42 Published online by Cambridge University Press

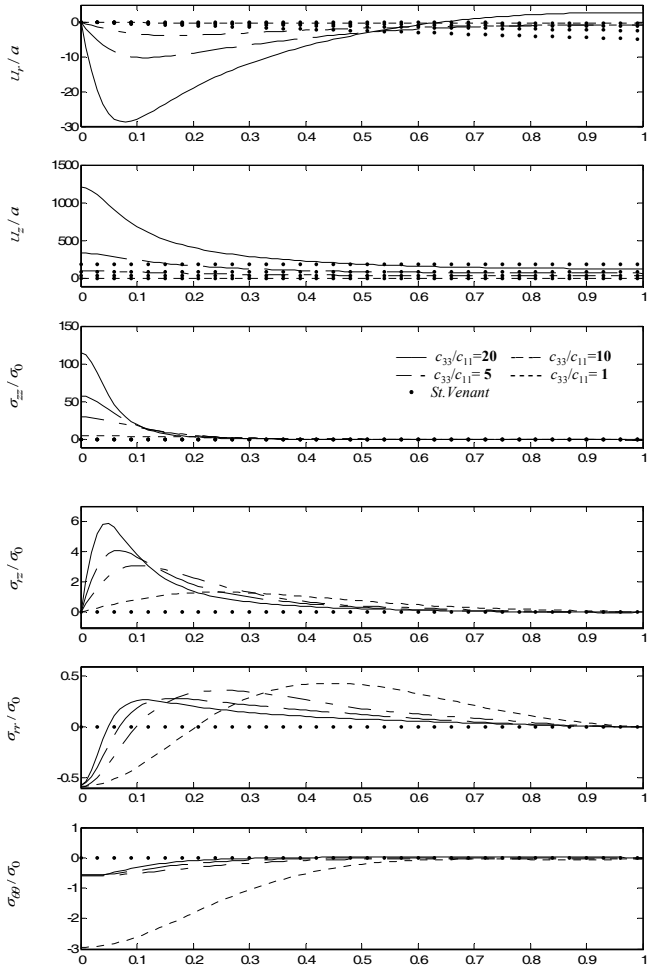


Fig. 7 Radial variations of displacements and stresses at $z = 9.5a$, under P

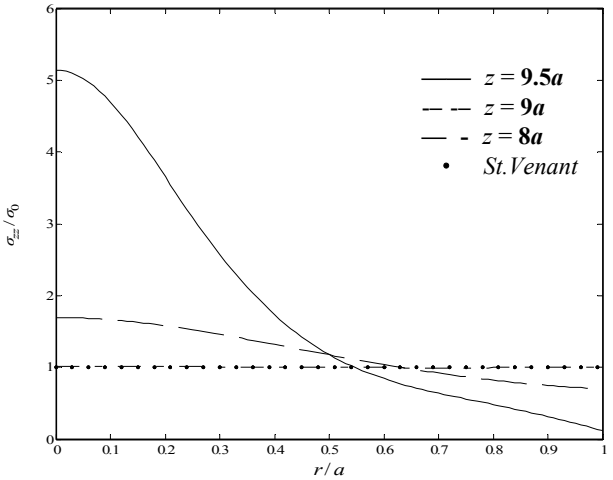


Fig. 8 Radial variations of normal stress σ_{zz} at $z = 8a$, $9a$, $9.5a$, under P at $z = 10a$

show that the end effect is significant but confined to a local region near the base of the cylinder where the end plane is perfectly bonded. The stress field depends on the axial stiffness, the distribution of the applied forces and the fixing manner. As the axial stiffness increases, the end effect on the displacement and stress state in the cylinder under the extension increases at the loaded end but decreases at the bonded end. Except near the ends, the deformations and stress distributions across the section are uniform as those given by the Saint-Venant solution throughout the cylinder.

The stress distribution near the ends of the cylinder depends upon how the axial load is applied. For an isotropic cylinder under extension, the Saint-Venant solution may be used with good accuracy at any point which is a diameter away from the ends, where the stress distribution in the cylinder may be assumed uniform and independent of the distribution of the applied loads.

ACKNOWLEDGMENTS

The work is supported by the National Science Council of Taiwan, ROC through grant NSC NSC99-2221-E-006-067-MY3.

REFERENCES

1. Timoshenko, S. P. and Goodier, J. N., *Theory of Elasticity*, 3rd Ed., McGraw-Hill, New York (1970).
2. Lekhnitskii, S. G., *Theory of Elasticity of an Anisotropic Body*, Mir, Moscow (1981).
3. Tarn, J. Q., "A State Space Formalism for Anisotropic Elasticity, Part II: Cylindrical Anisotropy," *International Journal of Solids and Structures*, **39**, pp. 5157–5172 (2002).
4. Tarn, J. Q., Tseng, W. D. and Chang, H. H., "A Circular Elastic Cylinder Under its Own Weight," *International Journal of Solids and Structures*, **46**, pp. 2886–2896 (2009).
5. Hildebrand, F. B., *Methods of Applied Mathematics*, 2nd Ed., Prentice-Hall, Englewood Cliffs, New Jersey (1965).
6. Zhong, W. X., *A New Systematic Methodology for Theory of Elasticity* (in Chinese), Dalian University of Technology Press, Dalian, China (1995).

(Manuscript received May 13, 2010, accepted for publication October 5, 2010.)

https://doi.org/10.1017/jmech.2011.42 Published online by Cambridge University Press